Slovak University of Technology in Bratislava
Faculty of Materials Science and Technology in Trnava

ARUN GOPINATHAN

Offprint of Dissertation Thesis

Composite panels with aluminum foam skeleton for heat storage

for being awarded the academic degree (Doctor ("philosophiae doctor", abbrev. as "PhD.")

in PhD. study programme: Advanced Materials and Material Design
in study branch: Mechanical Engineering
Training workplace: Institute of Materials and Machine Mechanics of the Slovak Academy of Sciences
form of study: Full-time

Trnava 2022

STU

Dissertation Thesis was elaborated at: Institute of Materials and Machine Mechanics of the Slovak Academy of Sciences

Submitted by: **Arun Gopinathan**
Institute of Materials and Machine Mechanics of the Slovak Academy of Sciences
Dúbravská cesta 9, 841 04 Bratislava

Supervisor: **Dr. Ing. Jaroslav Jerz.**
Institute of Materials and Machine Mechanics of the Slovak Academy of Sciences
Dúbravská cesta 9, 841 04 Bratislava

Reviewers:

Offprint was sent on: 2022.06.02

Defence of Dissertation Thesis will be on **at** **o´clock**.

at Faculty of Materials Science and Technology in Trnava Jána Bottu 2744/24, 917 24 Trnava Slovakia

prof. Ing. Miloš Čambál, CSc.
Faculty Dean

ABSTRAKT

Výstavba a údržba obytných budov predstavuje 36 % zo všetkých emisií CO_2 v EÚ (Európskej únii). Na dekarbonizáciu stavebných materiálov je najlepšie integrovať zdroje tepelnej energie do energeticky efektívnych budov. Materiály s fázovou premenou (Phase Change Materials – PCMs) sú jednoducho vintegrovateľné médium pre akumuláciu tepla v budove. Hlavným cieľom tejto práce je navrhnúť, vyvinúť a experimentálne overiť riešenie využitia práškovo-metalurgicky pripravenej hliníkovej peny s pórmi vyplnenými materiálom s fázovou premenou ako teplonosného média pre aplikácie akumulácie tepla. Práca je rozdelená do troch fáz: štúdium vplyvu rýchlosti prenosu tepla hliníkovej peny; štúdium termofyzikálnych vlastností vybraných materiálov s fázovou premenou a štúdium kompatibility hliníkovej peny impregnovanej materiálmi s fázovou premenou. Vnútorná štruktúra peny súvisiaca s pórovitosťou, ktorá rozhoduje o rýchlosti prenosu tepla, zohráva významnú úlohu pri akumulácii teplnej energie. Speniteľný polotovar z dvoch rôznych hliníkových zliatin (Al zliatiny 1050 a 5083) s 0,15 hm. % a 0,05 hm. % speňovadla (prášok TiH_2), bol pripravený zhutnením a extrúziou za tepla do tvaru vzoriek rozmerov 20 × 40 × 5 mm^3. Vzorky hliníkovej peny s rozmermi 40 × 40 × 5 mm^3 sa skúmali so zdanlivými hustotami 0,742 g/cm^3, 1,624 g/cm^3, 1,721 g/cm^3 a 1,726 g/cm^3. Vnútorná štruktúra peny bola charakterizovaná röntgenovou tomografiou. 3D model vnútornej pórovitej štruktúry vzoriek hliníkovej peny bol vytvorený pomocou rezov röntgenovej tomografie prostredníctvom techník spracovania obrazu na analýzu metódou konečných prvkov. Získané numerické výsledky pre rýchlosť prestupu tepla a efektívnu tepelnú vodivosť vyvinutých náhradných modelov odhalili vplyv pórovitosti a rozloženia stien pórov pri určovaní tepelného toku vo vnútornej štruktúre peny. Zistilo sa, že veľkosť pórov a ich distribúcia určujú rýchlosť tepelného toku v celej penovej štruktúre. Zjednodušené modely Bruggemanna a Russella môžu predpovedať vynikajúce výsledky efektívnej tepelnej vodivosti peny v celom rozsahu pórovitosti (8 % – 70 %). Skutočná štruktúra peny bola charakterizovaná rastrovacím elektrónovým mikroskopom (SEM) a porovnávala sa s vyvinutými náhradnými modelmi. Potvrdilo sa, že vývoj 3D modelu prostredníctvom techniky spracovania obrazu je obmedzený na modelovanie pórov s veľkosťou nad 100 µm. Termofyzikálne vlastnosti organického materiálu s fázovou premenou, akým sú kokosový olej (teplota topenia, T = 25 °C) a komerčne dostupný PCM Rubitherm RT28HC (teplota topenia, T = 27 – 29 °C), sa analyzovali pomocou metódy T-history. Ako referenčný materiál sa použila destilovaná voda. Pri experimentoch sa brali do úvahy rôzne kritériá, ako sú výhrevné/chladiace médium, veľkosť testovanej vzorky, poloha testovacej skúmavky, teplotný gradient a umiestnenie termočlánku na zaznamenávanie teploty PCM. Testy preukázali, že experiment uskutočnený na vzduchu s vertikálnym usporiadaním experimentálnych skúmaviek spĺňa podmienku Biotovho čísla (Bi < 0,1). Experimentálne zistené latentné teplo topenia RT28HC (242,004 kJ/kg) je vyššie ako u kokosového oleja (71,15 kJ/kg). Tepelná vodivosť RT28HC je zároveň o 45 % nižšia v pevnom stave a o 69 % nižšia v tekutom stave ako tepelná vodivosť kokosového oleja. Okrem toho sa v oboch PCM skúmal efekt podchladenia, pričom sa zistil stupeň podchladenia 0,1 – 0,7 °C u RT28HC a stupeň podchladenia 2,7 – 3,1 °C u kokosového oleja. Podchladenie je výsledkom slabej nukleácie a zníži sa, keď sa zníži teplotný

gradient chladiaceho cyklu. Boli vykonané ponorné a tepelné testy penového hliníka impregnovaného PCM, ktoré sa vykonali zahrievaním na 40 °C a ochladzovaním na 3 °C (rýchle chladenie) a 22 °C (izbová teplota). Trom vybraným vzorkám peny (30 × 10 × 7 mm^3) sa odkryli steny pórov. Dve vzorky sa podrobili pomalému chladeniu a jedna vzorka rýchlemu chladiacemu testu. Objem PCM vo vnútri nádoby bol nastavený na 35 % a 75 %. Po vykonaní testov rýchleho aj pomalého chladenia výsledky ukázali zanedbateľné poškodenie steny pórov v dôsledku objemovej expanzie. Zistilo sa 5 % časové oneskorenie, keď sa hliníková pena vložila do skúmavky obsahujúcej PCM. Okrem toho hliníková pena, do ktorej je naakumulované teplo, inhibuje nukleáciu, čo výrazne znižuje podchladenie. Nerovnomerný tepelný tok na tenších stenách pórov vedie k pomalšiemu topeniu PCM, čo potvrdzujú to aj výsledky numerickej štúdie. RT28HC v penovom hliníku vykazuje 5% časové oneskorenie zmeny fázy. Okrem toho absorpcia tepla hliníkovou penou znižuje podchladenie inhibíciou nukleácie. Nerovnomerný tepelný tok na tenších stenách pórov spomaľuje tavenie PCM, čo potvrdzujú výsledky numerickej štúdie. Pri teste tepelnej účinnosti sa vzorka Al peny (13,58 g) impregnovaná RT28HC (0,12 g) zahrievala a ochladzovala (ΔT = 28 °C). Testovaním hliníkovej peny s PCM a bez neho sa zistilo oneskorenie 1190 s. Z výsledkov vyplýva, že Al pena impregnovaná PCM uchováva o 11,28 % viac energie. RT28HC s penou zo zliatiny Al 1050 (40 – 50 % pórovitosť) s 0,05 % hm. TiH_2 zlepšuje akumuláciu tepla a je vhodná pre vnútorné aplikácie. Navrhuje sa riešenie na zabránenie úniku, ktoré si vyžaduje ďalšie štúdium pre praktické aplikácie. Pri teste tepelnej účinnosti sa vzorka z penového hliníka (hmotnosti 13,58 g) impregnovanej RT28HC (0,12 g) zahreje a ochladzuje (ΔT = 28 °C). Získaný graf testovaním vzorky penového hliníka s PCM a bez neho ukazuje oneskorenie uvoľňovania tepla o 1190 s. Zistilo sa, že vzorka penového hliníka impregnovaná PCM uchováva o 11,28 % vyššie množstvo energie. Kombinácia PCM RT28HC s hliníkovou penou (40 – 50 % pórovitosť) vyrobená zo zliatiny Al 1050 s 0,05 hm. % TiH_2 poskytuje efektívne riešenie na dosiahnutie lepšieho akumulovania tepla pre vnútorné aplikácie. Navrhuté je aj vhodné riešenie prevencie úniku PCM zo štruktúry penového hliníka, ktoré však vyžaduje ďalšie rozšírené štúdium za účelom jeho využitia v praktických aplikáciách.

Kľúčové slová: penový hliník, prášková metalurgia, akumulácia tepla, materiály s fázovou premenou

ABSTRACT

The construction and maintenance of residential buildings account for 36% of CO_2 emissions in the EU(European Union). Integrating thermal energy storage sources in energy-efficient buildings is best to decarbonize building materials. Phase-change materials (PCM) make an easy-to-integrate heat storage medium with the building. The present work aims to suggest, develop, and experimentally verify the solution of using powder-metallurgically prepared aluminium foam as a heat transfer medium for PCM-based heat storage applications. The entire work is divided into three phases: studying the heat transfer rate of aluminium foam, the thermophysical properties of selected PCMs, and the compatibility of PCM-impregnated aluminium foam. The internal structure of the foam formation, which determines heat transfer rate, affects thermal energy storage performance. The foamable precursor of two different aluminium alloys (Al-1050 and Al-5083) with 0.15 wt.% and 0.05 wt.% TiH_2 powder is prepared by extruding mixed powder compacts to a volume of 20 × 40 × 5 mm^3. Among the produced aluminium foam, the internal structure of the four foams (40 × 40 × 5 mm^3) with apparent densities of 0.742 g/cm^3, 1.624 g/cm^3, 1.721 g/cm^3 and 1.726 g/cm^3, are characterised by X-ray tomography. Image processing technique is adopted to develop the foam surrogate model for finite element analysis. One-dimensional steady-state thermal analysis is performed, which reveals the influence of porosity, struts, and pore walls on heat flow in the foam's internal structure. The numerical data are then validated against analytical predictions (based on various correlations) of thermal conductivity. The simplified models of Bruggemann and Russell and the parallel series model better predict foam's effective thermal conductivity across its porosity range (8% -70%). SEM analysis shows that image processing can only model pores above 100 µm. Further, the modified T-history method characterizes the selected organic phase change material such as coconut oil (T_m = 25 °C) and RT28HC (T_m = 27-29 °C). Distilled water is used as a reference material. Various criteria are considered for experiments, such as heating/cooling medium, sample quantity, test tube alignment, temperature gradient and thermocouple placement to record PCM temperature. The results show that the investigation performed in air with vertical alignment meets the Biot number condition (Bi<0.1). The experiment with 15g (same mass) samples yields 10% lower results than a 20ml sample (same volume) selection due to the difference in convective length. RT28HC (242.004 kJ/kg) stores higher latent heat than coconut oil (71.15 kJ/kg) by processing the cooling curve. The thermal conductivity of RT28HC is 45 % lower in the solid-state and 69 % lower in the liquid state than coconut oil. In both PCMs, supercooling is studied, revealing a degree of 0.1-0.7 °C in RT28HC and 2.7-3.1 °C in coconut oil. The supercooling results from poor nucleation and is reduced when the cooling cycle temperature gradient is reduced. Thermophysical results are validated against literature and manufacturer data. The immersion and thermal performance tests of PCM-impregnated aluminium foam determine the compatibility of PCM and heat transfer medium. The immersion tests are performed by heating at 40°C and cooling at 3 °C (rapid cooling) and 22 °C (room temperature). Three foam samples (30 × 10 × 7 mm^3) are selected and cut to expose the pore walls. Two samples are subjected to slow cooling and one sample to a rapid cooling test. The PCM volume inside the container is set to 35% and 75%. After conducting both rapid and slow

cooling tests, the results show negligible pore wall damage due to volume expansion. Further, RT28HC with aluminium foam shows a 5%-time delay in phase change. Additionally, the aluminium foam's heat absorption reduces supercooling by inhibiting nucleation. Uneven heat flux at thinner pore walls slows PCM melting, validating numerical study results. In the thermal performance test, the Al foam sample(13.58g) impregnated with RT28HC (0.12g) is heated and cooled (ΔT=28 ℃). Testing Al foam with and without PCM reveals an 1190s delay. From the results, PCM-impregnated Al foam stores 11.28% more energy. Thus, Coupling RT28HC PCM with Al-1050 alloy foam (40-50% porosity) with 0.05 wt.% TiH_2 improves heat storage and is suitable for indoor applications. A leakage prevention solution is suggested, requiring further study for practical applications.

Keywords: aluminium foam, powder metallurgy, heat storage, phase change materials

PREFACE

Among the different methods, high porosity metal foams provide an effective way of improving PCM's performance. Porous metal foams possess high thermal conductivity, large surface area ratios concerning volume, and highly interconnected pore walls. Much research has been conducted to study the thermal conductivity of the metal foam and the influence of microstructure and porosity on the effective thermal conductivity of PCM embedded with metal foam composites. Phase-change kinetics is greatly influenced by the effective thermal conductivity of the PCM. When the effective thermal conductivity increases, the heat transfer rate increases, which increases the melting and solidification rate of the PCMs. The study of the porosity and microstructure of the foam on thermal conductivity is of interest because it influences the rate of evolution of the melt fraction. The primary study conducted involves (1) the study of the properties of the aluminium composite foam having pores interconnected with microcracks of different density and porosity levels, which influence the thermal conductivity of the foam, and (2) the progress of the solid and liquid phase change of the PCM is studied to evaluate the thermophysical properties of the PCM, and (3) the performance of the PCM impregnated aluminium foam for heat storage.

1. WORK PLAN

The research work is divided into three phases, and the whole work plan is shown in Figure 1.

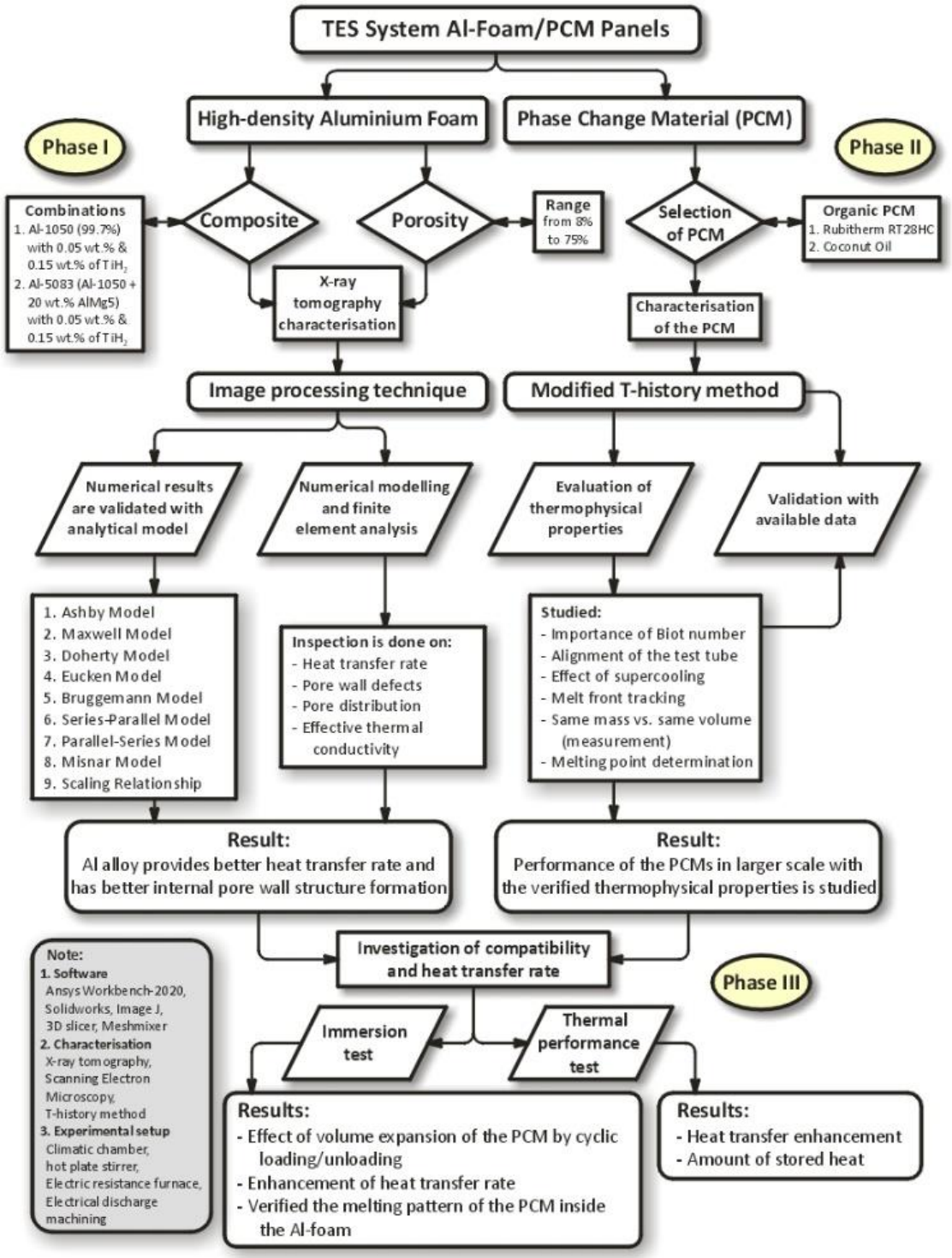

Figure 1. Thesis work plan

2. INVESTIGATION OF THE INTERNAL STRUCTURE OF ALUMINIUM FOAM

2.1 Methodology

Phase 1 follows the methodology of investigating the internal structure of the aluminium foam, which involves sample preparation, X-ray tomography characterisation, the image processing technique adopted to create the surrogate model, and numerical modelling and analysis.

2.1.1 Sample preparation

The powder metallurgical process produces aluminium foam samples according to the procedure described in Figure 2.

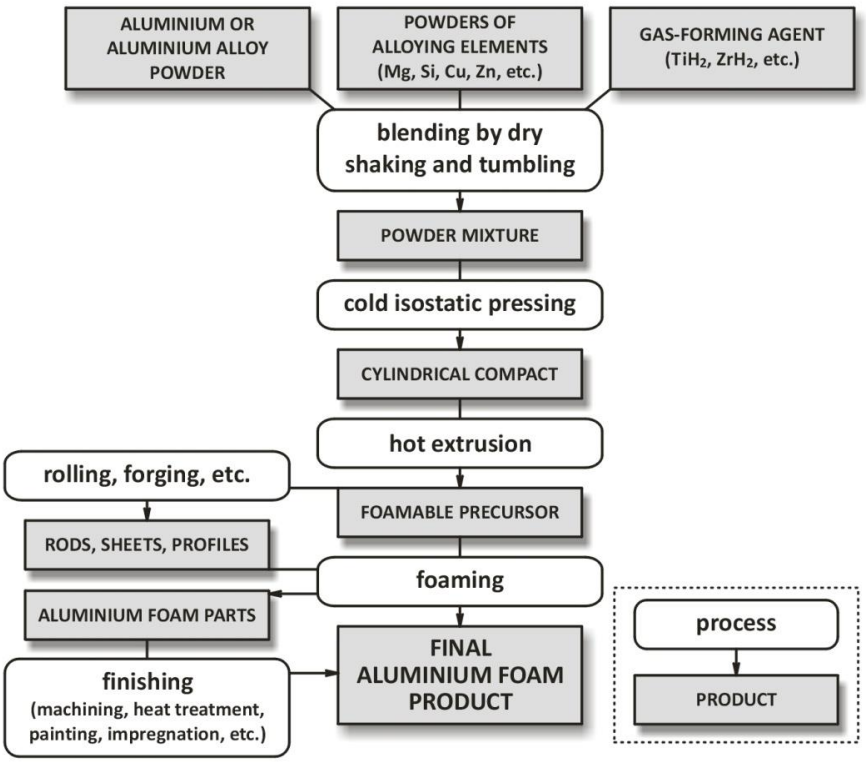

Figure 2. Schematic diagram of the production of aluminium foam by the PM method

2.1.2 Selection of powders

The samples are prepared from an aluminium powder of 99.7% purity with a particle size of <63 μm and AlMg5 with a particle size < 400 μm. The powder supplier KERAMETAL, Ltd., Slovakia, reports that the aluminium powder used in this study is composed of 99.7 wt.% Al, 0.11 wt.% Fe and 0.06 wt.% Si. The pre-alloyed AlMg5 powder (99.7 % purity with particle size < 400

μm) is supplied by Mepura (Austria). The solid thermal conductivity of Al (99.7 wt.% purity) chosen for the work is 225.3 W/(m·K). The solid thermal conductivity of AlMg5 chosen is 120 W/(m·K). The foaming agent TiH_2 is supplied by Chemetall (Germany), which belongs to grade U with a particle size ≤ 45 μm and a mean particle size d = 5 ± 1 μm. The fine-grained powder used to prepare a foamable precursor has been shown to significantly prevent the foam structure from collapsing during foaming when the precursor is allowed to melt. A foamable precursor is prepared to contain 0.15 wt.% and 0.05 wt.% of foaming agent, TiH_2 powder, to achieve a higher foam density with ease. The selection of the quantity of TiH_2 powder is based on the quality of foamable billets produced at the extrusion and pores formation, which can be achieved at foaming. The foam density is less with bigger pores when the foaming content is >0.15 wt.%. The poor pore formation occurs when the foaming agent is < 0.05 wt.%.

2.1.3 Production of foamable billets

The mixing of the metal powder and the blowing agent is significant for improving the quality of the aluminium foams with a uniform pore size distribution. The T2F model turbula mixer is acquired for the mixing process, and it occurs for 2 hours (average) for proper mixing of the powders. Cold isostatic pressing (CIP) aims to obtain a semi-finished compacted powder product, a green body with handling strength that can be further processed. At first, the powder mixture is compressed to cylindrical billets to achieve 70-80% of the theoretical density with the help of cold isostatic pressing. The billets are hot extruded to a rectangular profile of cross-section - 5 × 20 mm^2 (selected Al alloy with 0.15 wt.%) and 2 × 20 mm^2 (selected Al alloy with 0.05 wt.%). The extrusion temperature is fixed to 450 °C. The extrusion ratio is 28:1. The samples are foamed in a steel mould in an electric resistance furnace in the form of small square plates (40 × 40 × 5 mm^3) using the foamable precursor of dimensions 20 × 40 × 5 mm^3.

2.1.4 Production of Al foam

Ten samples of each Al-1050 alloy and Al-5083 alloy are foamed with 0.15 wt.% and 0.05 wt.% TiH_2 as the gaseous agent. Good reproducibility is achieved in the density range of 0.7 to 2.24 g/cm^3. Foaming is performed under various furnace temperatures from 730 °C to 690 °C. The precursor inside the steel mould is overheated when the furnace temperature is maintained at 730 °C. It leads to the poor quality of aluminium foams. Better foaming has been found by keeping the

furnace temperature at 720 °C and 690 °C. The corresponding time which is taken for the foaming is recorded.

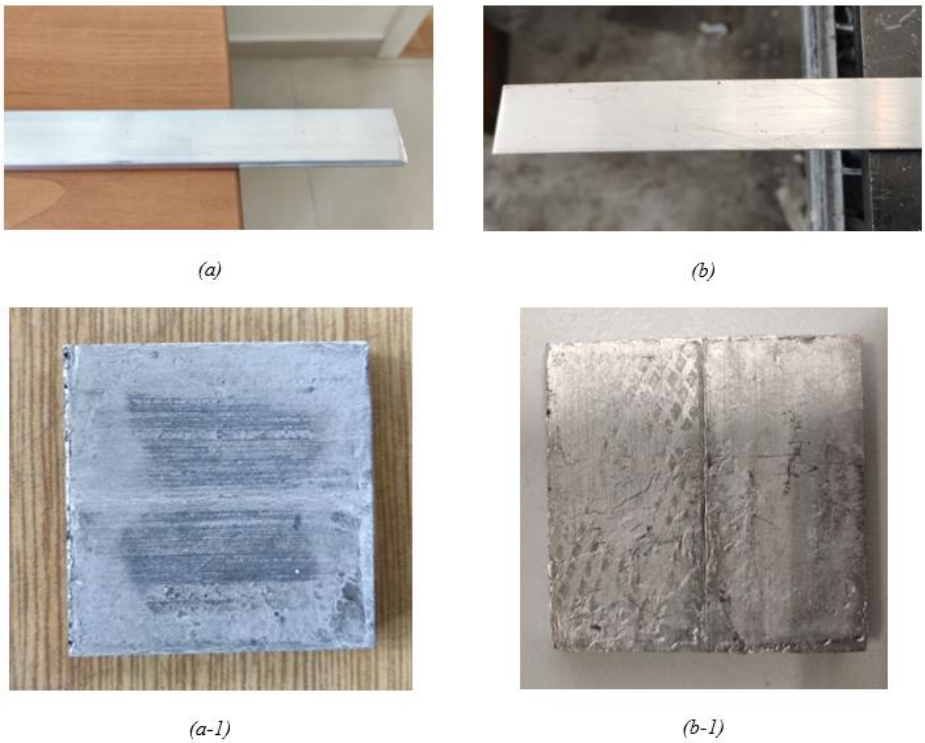

Figure 3. Foamable rectangular profile of cross-section (a) 5 × 20 mm², (b) 2 × 20 mm² and (a-1, b-1) aluminium foam sample prepared (40 × 40 × 5 mm³)

Table 1: Foaming Conditions and Structural Parameters of the Al Foam

Aluminium alloy	Sample	Composition of TiH_2 (wt. %),	Precursor weight, (g)	Furnace temperature, (°C)	Foaming time, (s)	The apparent density of the foam, ρ_r (g/cm^3)	Porosity (%)
Al-1050	A1	0.15	14.43	720	330	0.742	72.5
	A2	0.15	14.68	720	360	1.624	39.9
Al-1050	A3	0.05	15.53	690	489	1.721	36.25
Al-5083	A4	0.05	15.57	690	411	1.726	36.07

Four samples, A1, A2, A3, and A4, are chosen for the numerical investigation of all foamed models. The foaming conditions and the structural parameters are mentioned in Table 1.

2.1.4 X-ray tomography characterization

Observation of the structure is done using a Phoenix/X-ray Nonatom 180. CXZ device (Manufacturer - G & E, Institute of Materials and Machine Mechanics, Slovak Academy of Sciences, Bratislava, Slovakia). This approach is a suitable method to study the pore wall architecture and distribution of metal and pores. The slice images are made quantitatively. It helps to calculate the tortuosity of the different phases, density distribution, pores, and cell size distribution. The slice image view in three directions and the 3D view of the sample position A3, which is placed for X-ray tomography imaging, are shown in Figure 4.

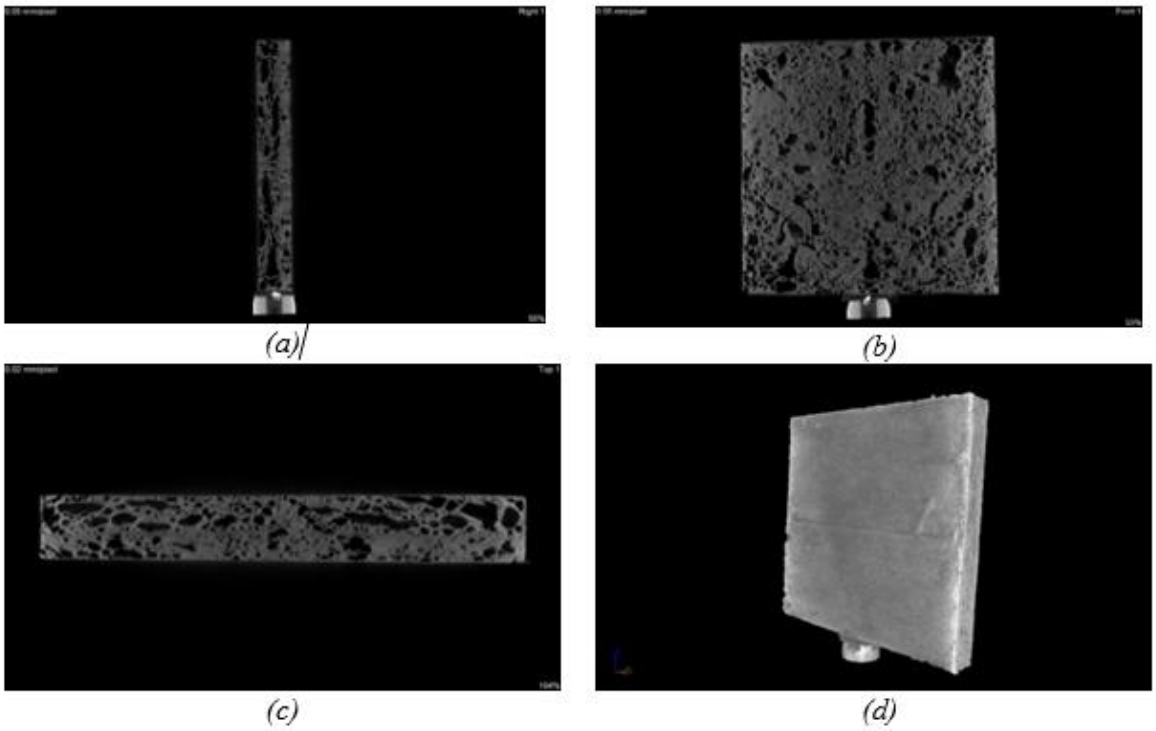

Figure 4. X-ray tomography images of the sample A3 (a) view along the X direction, (b) view along the Y direction, (c) view along the Z direction, and (d) 3D view of the real foam sample A3 (36.25 % porosity)

2.1.5 Image processing technique for developing the surrogate model

A 3D graphic model is produced from the X-ray slice images. It is achieved by detecting the edges of the images. For this study, 3D slicer software is utilised. In the section, the creation of the developed surrogate model is explained with sample A4. The surrogate model of dimensions

$7.5 \times 7.5 \times 5$ mm^3 is developed to simplify the computation time for investigating the structure with numerical modelling. The creation of the 3D model from the cropped slice images in the 3D slicer software is shown in Figure 5.

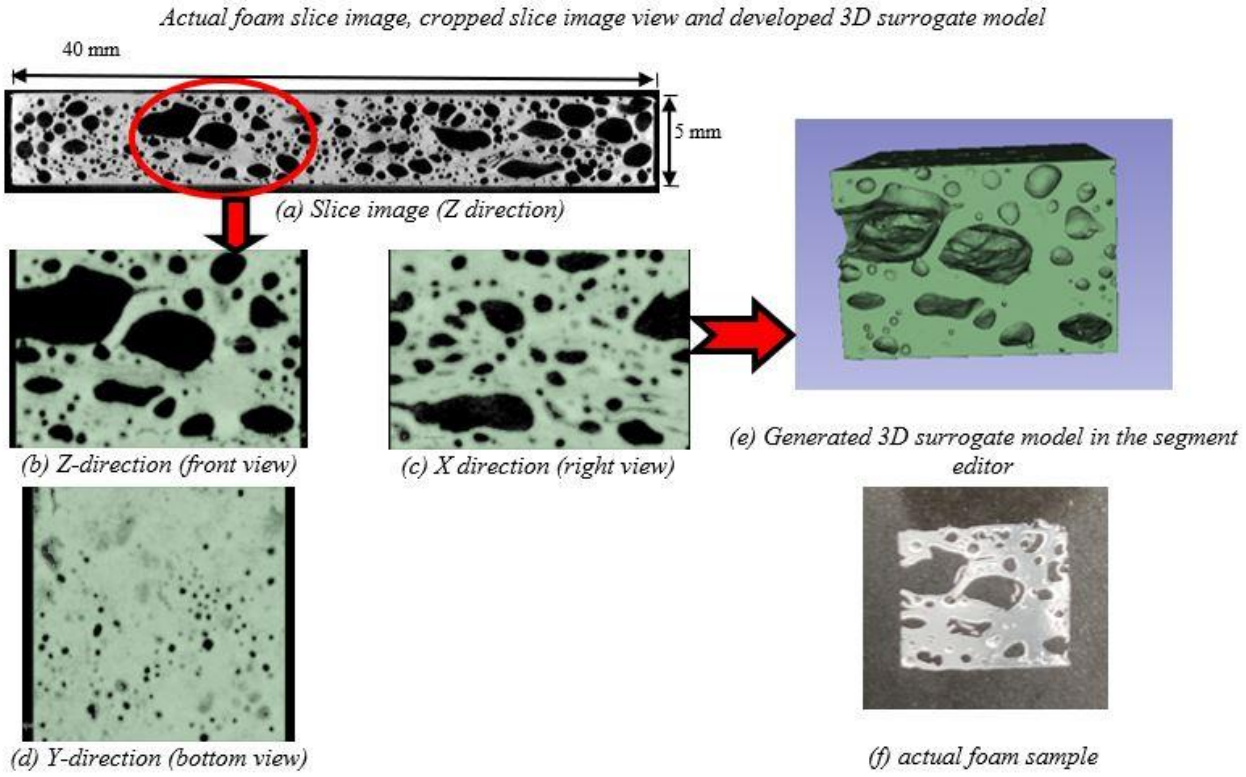

Figure 5. 3D surrogate model of the sample "A4" developed from the cropped slice image in 3D slicer software, (a) 78th slice image view made along the Z direction, the cropped slice image view along, (b) Z direction (front view), and (c) X direction (right side view), (d) Y direction (bottom view) (e) generated 3D surrogate model of the actual foam in segment editor module and (f) actual foam sample structure for comparison.

2.2 Results and Discussion

2.2.1 Effective thermal conductivity of the surrogate models

The reduced modelling procedure is applied to the A1 and A2 samples. The structure inside the foam is difficult to simulate, and the computation time takes longer. It can be avoided by splitting the whole foam sample into 16 sections of equal dimensions ($9.8 \times 9.8 \times 5$ mm^3 approx.). The crop volume module of the 3D slicer software is utilised for this purpose (same procedure mentioned in Figure 5). As the one-dimensional steady-state heat transfer is conducted, the thickness of the foam (5 mm) is kept constant for all the models. This approach helps determine

the function of foam struts, pores, and breakage of pore walls formed inside the closed-cell foam structure in the heat conduction process in a particular area. The temperature distribution of the aluminium foam is determined by performing a one-dimensional steady-state analysis along the direction of the foam model of a thickness of 5 mm with appropriate boundary conditions. The temperature on one side of the surrogate model is fixed at 63.85 ℃ and 22 ℃ on the opposite side. Steady-state thermal analysis is used to calculate the effect of steady thermal load on the system (shown in Figure 6). The investigation determines the temperature, thermal gradient, heat flow rate, and amount of heat flow that does not vary over time. The temperature contour of one of the foam surrogate models (A2 × 11) simulated in the Ansys workbench is presented in Figure 6.

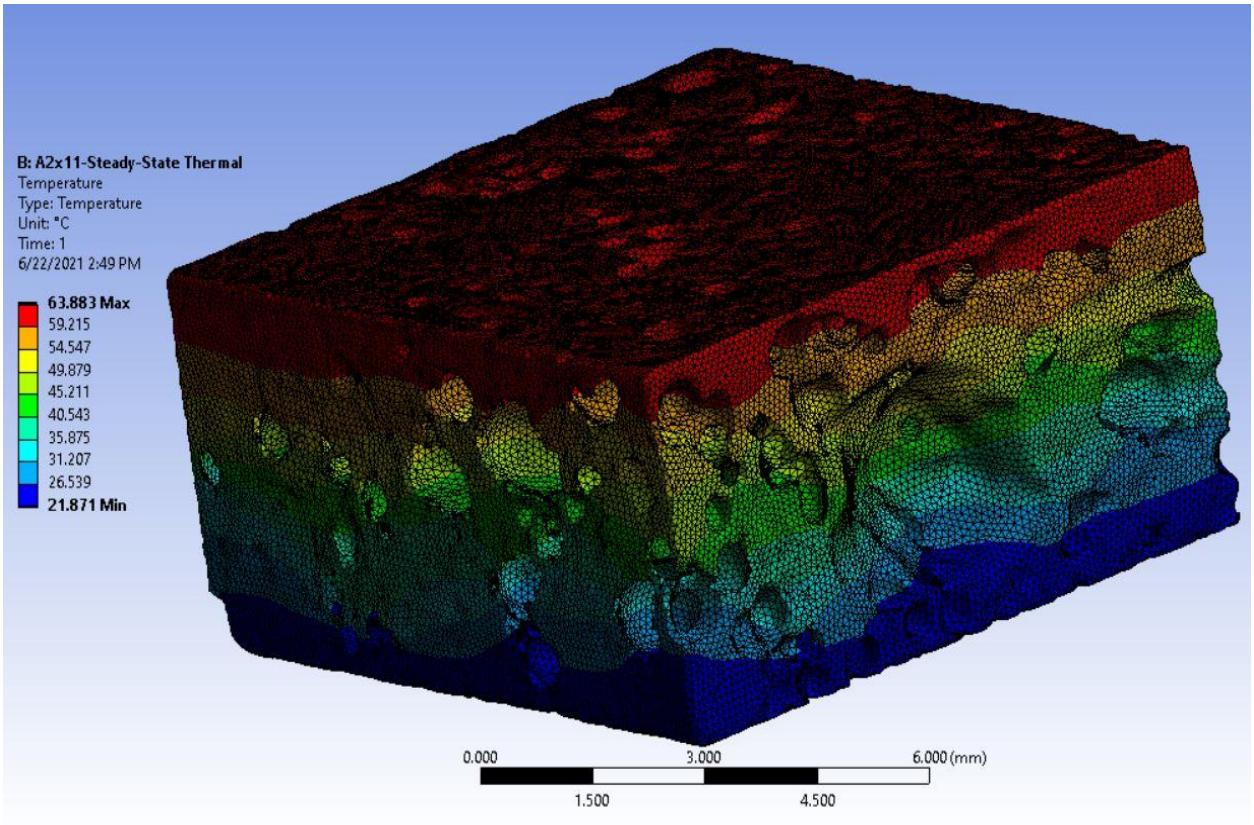

Figure 6. One dimensional steady-state thermal analysis of the foam model A2 × 11

The comparison of the numerical results obtained from 16 developed surrogate models and the results of mathematical models mentioned in the work plan (Figure 1) is shown in Figure 7.

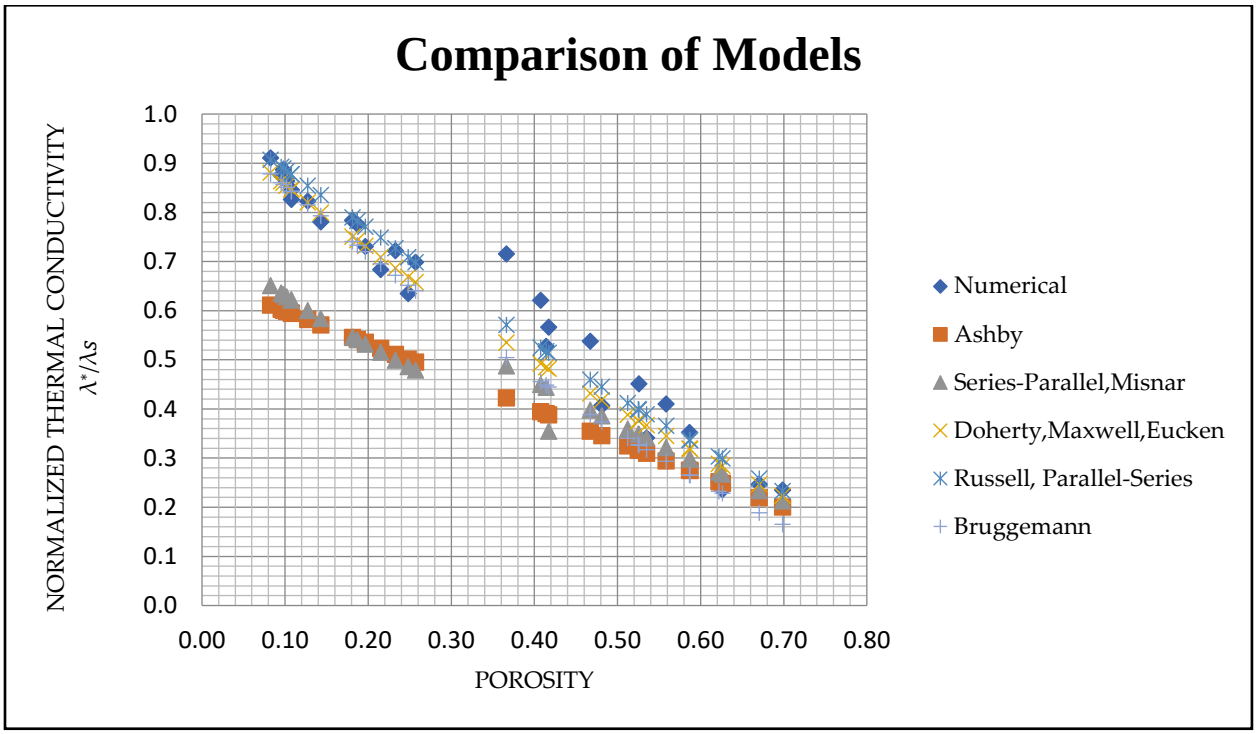

Figure 7. Normalised thermal conductivity predictions of the analytical models as a function of foam porosity in comparison with the numerical results ($\lambda_s = 225.3\ W/(m \cdot K)$)

2.2.2 Size and morphology of the pores

Most of the pore space area inside the closed-cell aluminium foam is spherical. It is closed fully or partially, in which the breakage of the walls and interconnection between the pores occurs. ImageJ image processing software is usually utilised to analyse pore size, spacing, and count. When the X-ray tomography images of the foam are examined, no pores of definite shape are found. The presence of pore wall ruptures is found in both samples. Predicting the distance of the wall of the pores with the X-ray tomography image is difficult. It is verified by finding the space of the pore wall in the X-ray slice image at the midsection of the sample with the help of ImageJ software. The same pore of the 3D model at the midsection is analysed in the SpaceClaim module of the Ansys workbench. A specific length difference is observed (see Figure 8). The measure tool of the SpaceClaim measures the distance between two vertices of the pore wall.

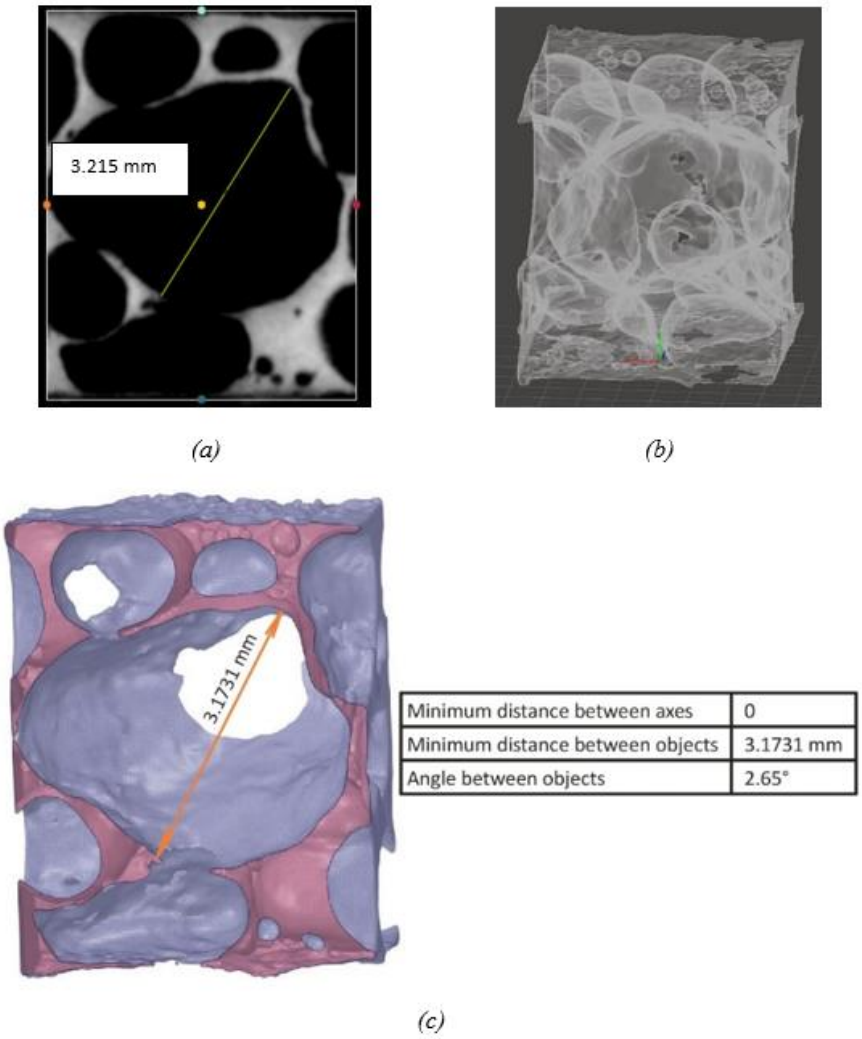

Figure 8. (a) Pore wall distance of 3.215 mm measured in ImageJ software of the sagittal image view of the mid-section slice image, (b) pore distribution and (c) pore wall distance of 3.1731 mm measured at the mid-section of the 3D model in SpaceClaim module of Ansys workbench

2.2.3 Reconstruction of actual foam and defects

When the foam samples are examined under the scanning electron microscope at a higher resolution, it has been found that considerable numbers of micro and nanopores are available in the structure, which is challenging to model with image processing. The structure obtained from the foam is shown in Figure 9. From the analysis made by comparing the 3d model developed and the exact foam under SEM, the possibility of modelling the pores is limited to above 100 µm. Moreover, some impressions or ruptures at the pore walls are limited to model in the 3d structure of the foam. The numerical simulation results reflect this difficulty in modelling the defects and pores on the micro-and nanoscales.

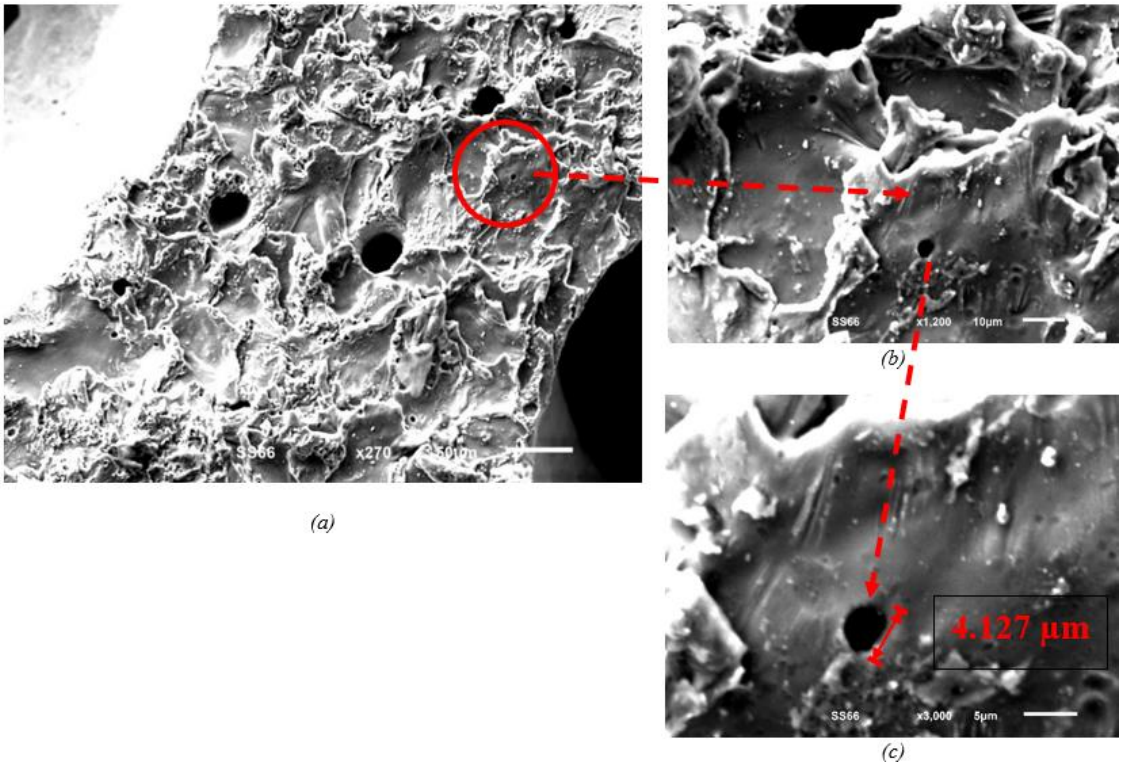

Figure 9. (a) Structure of the pore wall of the A4 sample at ×270 magnification, (b) the observation of the pore at ×1200 magnification and (c) the diameter of the pore of 4.127 µm observed at ×3000 magnification

The thermal conductivity of the foam dramatically increases when porosity is low. There are several reasons for the errors of the different models, especially for the higher porosity models, which lack the support of the present systematic research. Possible explanations for the error factors are related to the accuracy of the reconstruction process of the '. Stl' file, in which the minimum level of the detectable pore size is affected due to the distance between the slicing planes when the X-ray tomography image is made. In general, the higher resolution of X-ray tomography enables better modelling of foam irregularities and their influence on thermal conductivity. In addition to the porosity, the apparent thermal conductivity value depends on the pore's shape, the density distribution, the pore walls merging, and other geometric imperfections such as pore wall rupture with microcracks present pore wall misalignments, fractured walls, size variations of the pores, etc.

2.2.4 Influence of struts and thickness of the pore wall

The total heat flux has been analysed for each foam model. It helps to find the influence of the struts and the thin ligament distribution on the amount of heat transfer in addition to porosity.

The surrogate model created is different from the idealised representation of the model and has different strut thicknesses. Unlike the solid model showing a linear heat flux rate, the porous 3D models offer nonlinear heat flux rates inside the structure, which increase at the thin ligaments, at the merged surfaces of struts and nodes, and at the thin cell walls. As mentioned, the fused surfaces of the struts and nodes constitute many solid elements predominant in the structure of closed-cell foams. Heat conduction is limited to the small cross-sectional area of the strut, which is higher in the case of higher porosity foams where larger pores are more likely to be present with thin struts. It leads to a reduction in the average heat flux rate and the lower thermal conductivity of the foam. At the same time, a higher total heat flux rate has been found at the struts and the merged strut and node areas. It is the result of their lowe cross-sectional areas, as shown in Figures 10-a, b.

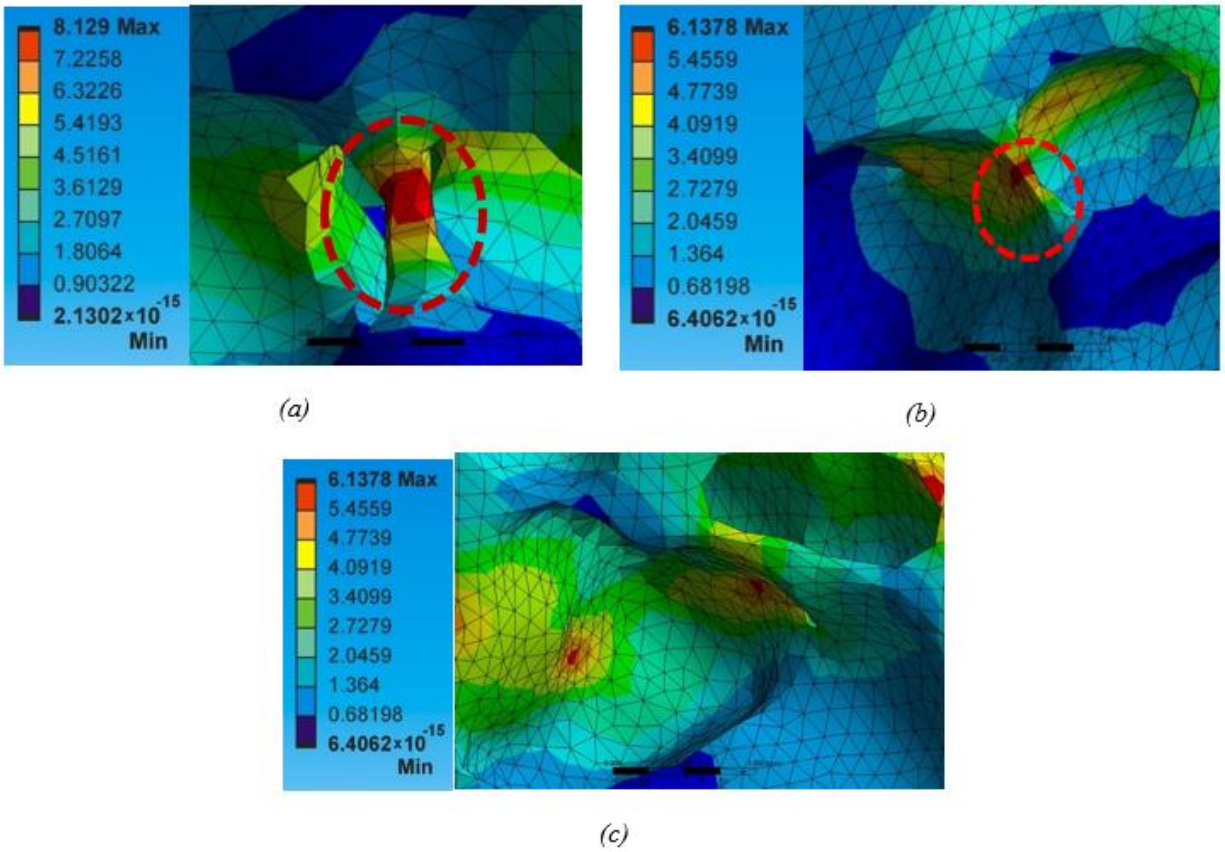

Figure 10. Maximum heat flux (W/mm^2) at (a) thin ligaments (A1 × 32) and (b) struts (A1 × 42), and (c) the heat flux distribution at the cell walls (A1 × 42)—52% foam porosity.

The thin ligament formation is low in the lower porosity foams. It leads to the linear heat flow occurring for most inside structures than in the higher porosity foams (Figure 10-c).

2.2.5 Formation of pores inside the foam samples

The 3d model of the foams developed from the X-ray tomography images of the four selected samples is observed with the help of Meshmixer. The pore evolution is shown in Figure 11. It has been found that the pores formed at the internal structure are spherical for A1, A2, and A3 models. It is developed from the alloy Al-1050. The higher porosity of the foams has bigger pores, with thinner pore walls having defects. The foam sample A4, made of Al-5083 alloy, has a limited number of macro-spherical pores compared to the other foam samples, limiting the PCM impregnation.

Furthermore, the thermal conductivity of the Al-5083 alloy is 53% lower than that of pure aluminium, restricting the usage for further consideration. Samples A2 and A3 give the possibility of bringing the heat eventually. The A3 sample has fewer micropores and offers a better internal structure with the minimal blowing agent (TiH_2) when comparing both cases. Thus, the pure Al-1050 alloy with 0.05 wt.% TiH_2 is considered to study PCM impregnation further.

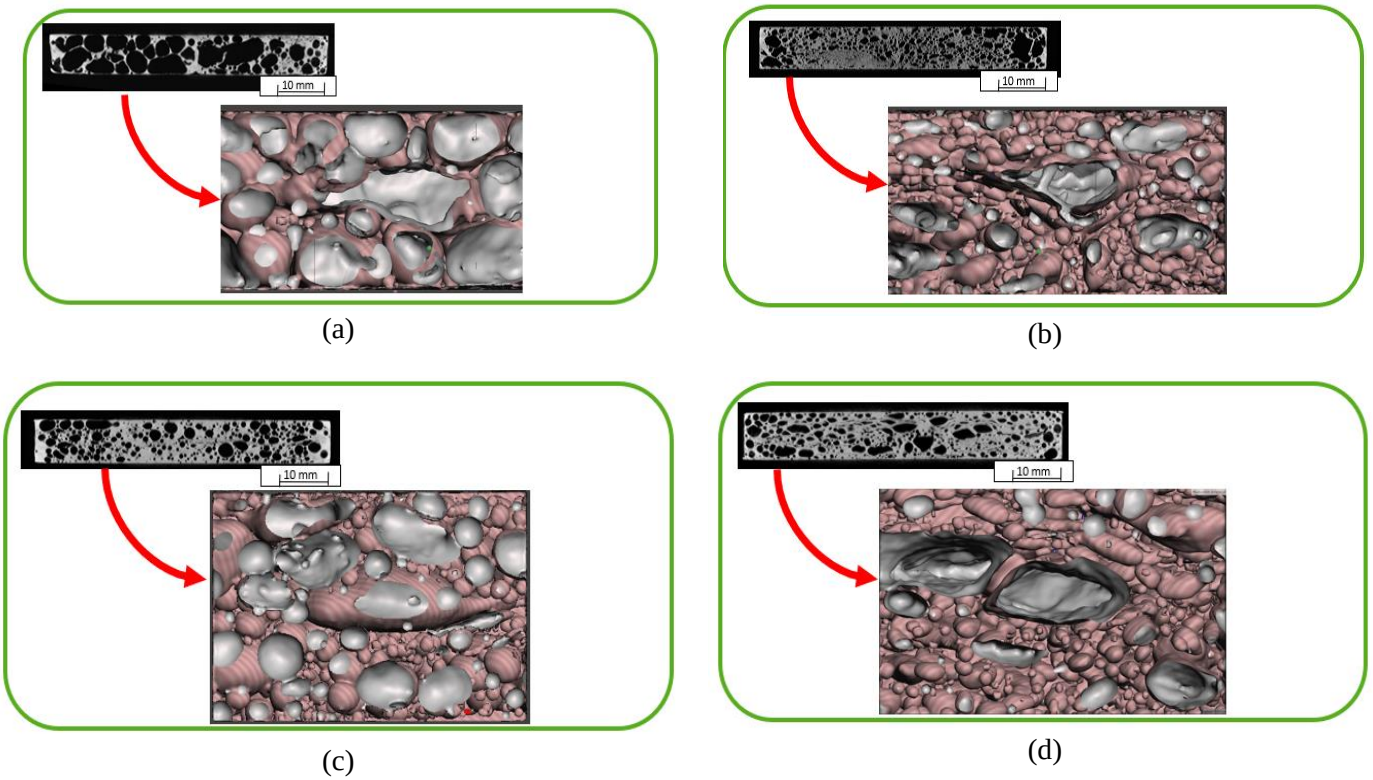

Figure 11. Pores distribution in the internal structure of the foam sample (a) sample A1 with 72.5% porosity, (b) sample A2 with 39.86% porosity, (c) sample A3 with 36.25 % porosity, and (d) sample A4 with 36.07 % porosity.

3. CHARACTERISATION OF THE PCM BY MODIFIED T-HISTORY METHOD

The T-history method is a method of analysing the thermal properties of materials by recording the heating and cooling cycle for a certain period. The heating and cooling cycle of the materials for investigation and the reference material of known thermal properties are recorded simultaneously. Water is the standard reference material chosen to test the sample in the temperature range of 0 ° C to 100 ° C. The obtained graphs are compared to find the melting, heat of fusion, the capacity of the material to store heat, and phase transition of the selected material for study.

Commercially available organic phase change materials, such as RT28HC(Paraffin wax manufactured by Rubitherm) and coconut oil, are used for this study. The experimental setup consists of the following elements:

- Six test tubes are made of borax glass, in which three are filled with the same mass of the samples, and the other three are filled with samples of the same volume.
- hot plate stirred to heat the glass flask containing 800ml of water (non-insulated)
- Climatic chamber in which the thermostat with continuous cold-water circulation cools the inside chamber
- Eight thermocouples with a 1 mm diameter
- Measurement system containing omega thermometer

3.1 Experiment methodology

The experiment is carried out following the original T history method. The original T history method is followed by heating the container containing samples to a temperature above the melting point of the PCM. Once the steady-state is achieved, it is immediately exposed to the cooling atmosphere, either a cooling water bath or an insulated cooling chamber, to cool down. The temperature range should be high to achieve the phase transition.

The experimental arrangement of the heating and cooling cycle is shown in Figure 12,

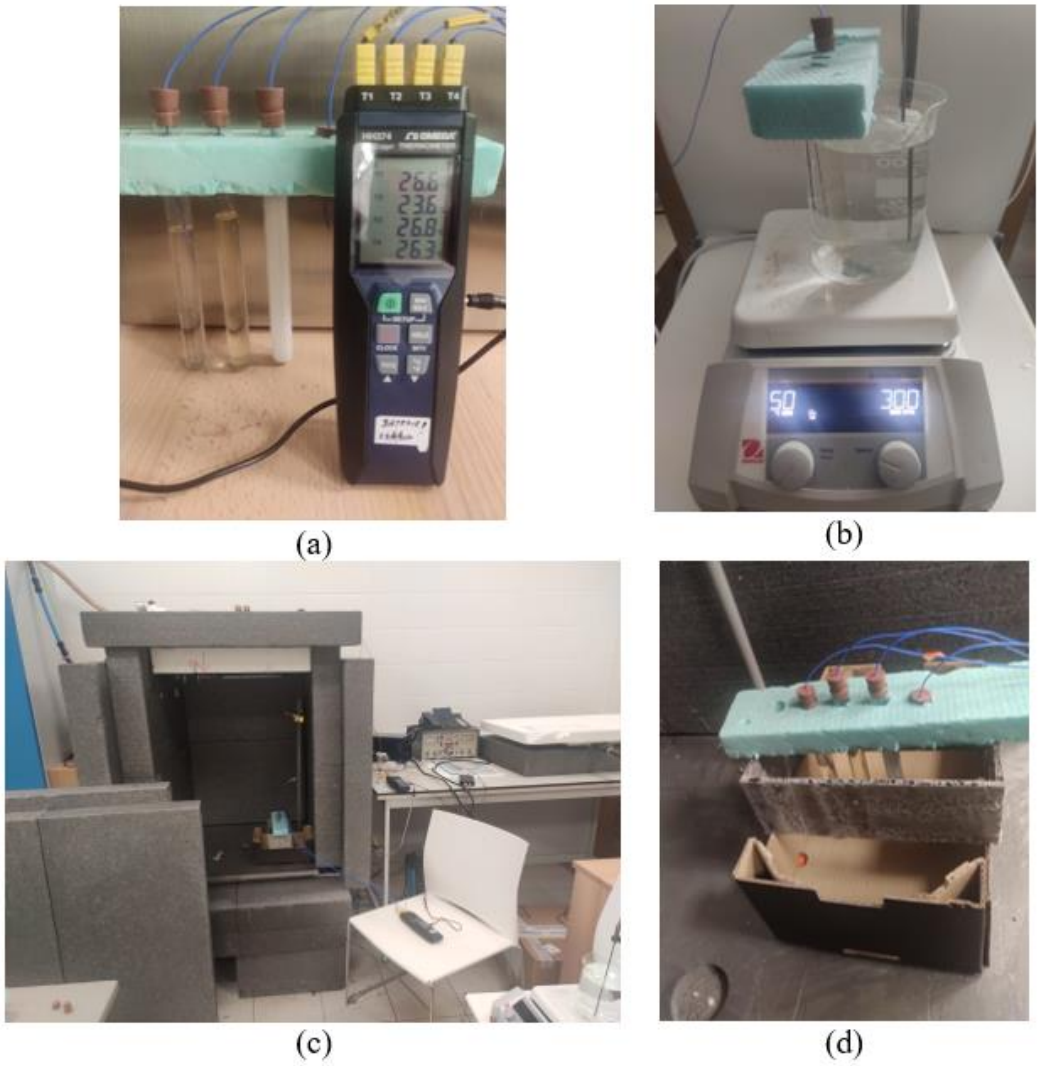

Figure 12. (a) Test tube filled with distilled water, coconut oil, and RT28HC relates to the thermocouple, (b) Omhaus hot stirrer plate containing the flask filled with 800ml of distilled water, (c) View of arrangement inside the climatic chamber, and (d) samples mounted inside the chamber at the bottom

The following factors are considered in the analysis of their influence on the thermophysical properties of the chosen PCMs.

- Importance of the Biot number to apply the lumped capacitance method
- Quantity of the sample for study (same mass vs the same volume)
- Alignment of the test tube for the heating and cooling cycle
- Placement of the thermocouple
- Melting fraction
- Effect of supercooling

The obtained thermophysical properties such as melting point, sensible heat at the solid and liquid phase of the PCM, latent heat storage at phase change, and the thermal conductivity of the PCMs are validated against the available data from the manufacturer and literature.

3.2 Results and discussion

3.2.1 Thermophysical properties of PCMs

The calculation of the Biot number should satisfy the condition (Bi<0.1) to use the lump capacitance method to find the thermophysical properties of the PCM. The air is the suitable medium for conducting the cooling and heating cycle from the various analyses. When the alignment of the container is undertaken, the characteristic length in which the heat convection occurs is considered. When the cooling process is deemed horizontal, heat transfer occurs from bottom to top, and the diameter of the test tube acts as the convective length of the tube. The obtained Biot number value is more significant than 0.1. When cooling is performed in the vertical position, the length of the test tube filled with the sample is considered the characteristic length. Among the different combinations, the vertical alignment of the container (test tube) is suitable that satisfies the condition Bi<0.1.

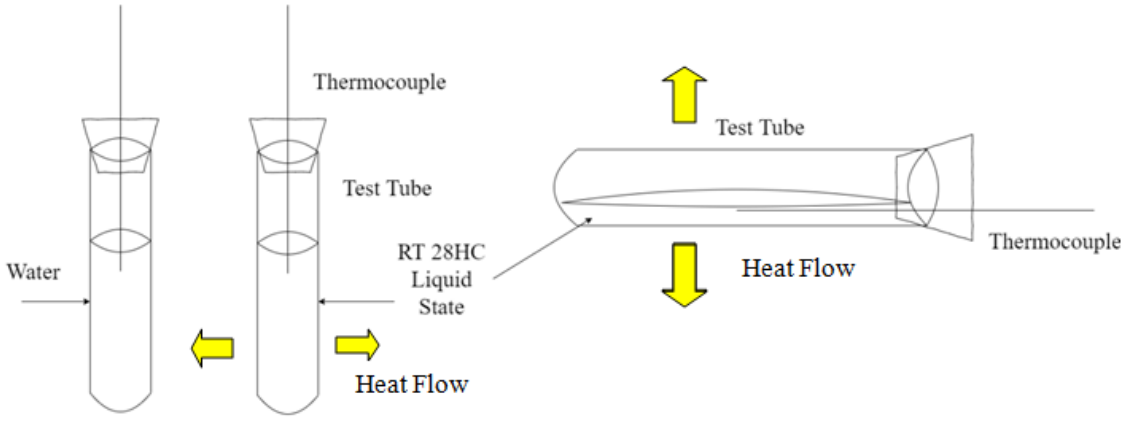

Figure 13. Position of the test tube and heat flow

Moreover, the same volume sample is suitable for the experiment since the same mass condition (different volume due to density difference) has different convective lengths, which leads to quick cooling/ heating of the reference material (water). It leads to a lower value of the

thermophysical properties. The representation of the test tube position and heat flow is shown in Figure 13.

Thus, the experiment is carried out in the vertical position under the same volume condition (20ml) under air as the medium. The heating cycle is not suitable for data interpretation since the noisy curve is obtained. The cooling cycle is ideal for predicting thermophysical properties. The thermophysical properties of the PCMs -RT28HC and coconut oil obtained are validated against the available data and presented in Table 2.

Table 2: Thermophysical properties of RT28HC and coconut oil in comparison with manufacturer data and the literature

PCM	Obtained results	Melting Temperature, (°C)	Specific heat capacity, C_p (liquid/solid) (kJ/kg.K)	Heat of fusion, H_m (kJ / kg)	Thermal conductivity ,(liquid/solid) λ_{pcm} (W/ m·K)
RT28HC	Manufacturer data	27-29	2	250	0.2
	Experimental	27.6	1.95/2.38	242.004	0.175/0.226
Coconut Oil	Literature	17-24	2.25/3.29	72	0.321
	Experimental	19.7	2.385/2.42	71.15	0.253/0.5

The image processing technique observes the melting fraction of the PCM in the range of 0-1(presence of liquid PCM inside the test tube). The experiments' results prove that the Biot number is influenced by the temperature gradient, convective length, and medium in which the heating and cooling are performed. The thermocouple placement inside the test tube is essential for accurately measuring the temperature since the heat acquired by the thermocouple affects the nucleation growth in the cooling cycle. It leads to the supercooling trace on the cooling curve. In addition, the effect of supercooling due to poor nucleation is observed in the range of 0.1-0.7 ° C for RT28HC and 1.7 -3.1 ° C for coconut oil. It can be reduced by reducing the nucleation growth rate by keeping the lower temperature gradient of the cooling cycle.

4. PORE WALL STRUCTURE INTERACTION WITH PCM

4.1 Immersion test

In this section, PCMs embedded in aluminium foam are investigated. The pore walls of the aluminium foam samples produced are embedded with PCMs such as RT28HC and coconut oil. The powder-metallurgically produced high-density aluminium foam from the foamable precursor of aluminium alloy Al-1050 with 0.05 wt.% TiH_2 is considered for the present study. The testing methodology follows the immersion test used to investigate the corrosion. It involves

- the preparation of samples,
- morphology of the pore walls examined
- Cleaning of the samples after being taken out of the PCM and dried inside the oven for 4 hours
- evaluation of the structure before and after exposure to volumetric expansion of the PCM

The experiment is performed twice.

- Investigating two Al foam samples of different masses by immersing inside the PCM container for six weeks, and the heating and cooling cycle is completed under room temperature (Temperature gradient, ΔT=18 ℃).
- investigating Al foam sample by immersing inside the test tube containing PCM and allowing it to 125 cycles of cyclic loading/unloading (Temperature gradient, ΔT=42 ℃)

4.2 PCM impregnated aluminium foam

In this section, the aluminium foam sample produced is impregnated with RT28HC and the cooling cycle undergone by the sample is presented in detail. Based on previous findings of thermophysical properties, foam samples made of Al-1050 and PCM RT28HC are selected to study their compatibility in the construction of PCM-based TES systems. The foam sample of dimension 40 × 40 × 5 mm^3 is produced, and the mass of the sample obtained is 13.91 g. Al foam is drilled from the top to a depth of 4 mm and impregnated with RT28HC PCM. The Al foam sample is heated with the help of a hot stirrer plate to 45 ℃ and then abruptly introduced inside the climatic chamber maintained at 17 ℃. The sample is insulated to allow heat transfer to occur

one-dimensional. The foam cooling cycle is recorded by placing the thermocouple 5 mm from the sides of the tube. The experimental arrangement is shown in Figure 14 below.

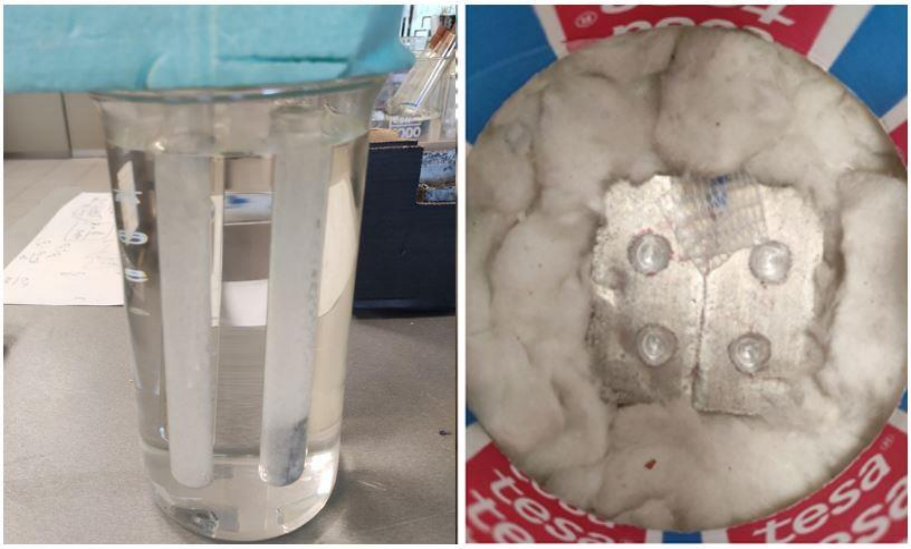

(a) (b)

Figure 14. (a) Arrangement of the test tube containing PCM (with and without Al foam) (b) Drilled Al foam for PCM impregnation

4.3 Results and Discussion

SEM images obtained before and after the experiment with a 75% volume of a test tube filled with RT28HC are shown below (Figure 15).

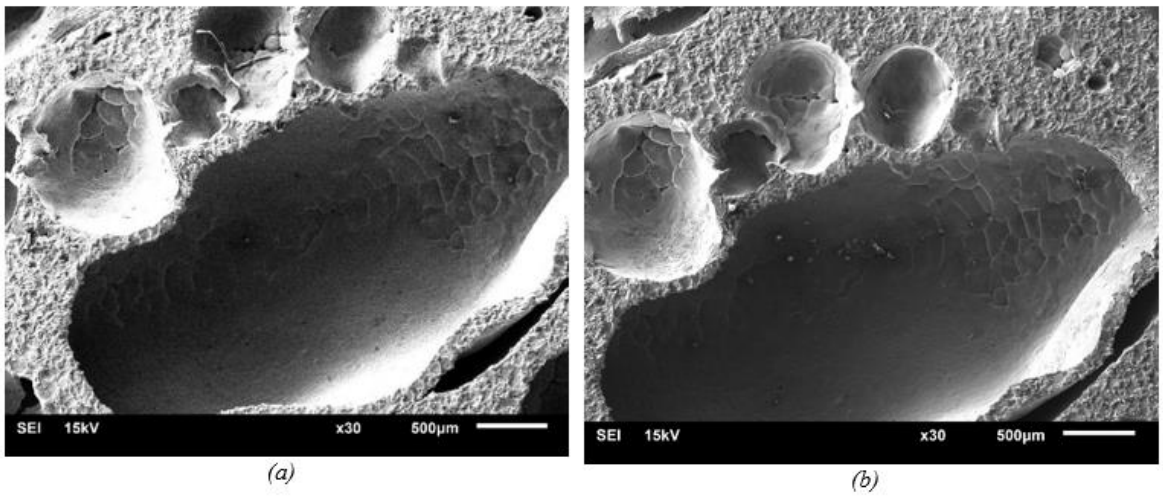

(a) (b)

Figure 15. SEM image of the pore wall made before (a) and after (b) subjected to the rapid heating/cooling 125 cycles

In both experiments performed before and after modification, negligible pore wall damage has been found. It proves the reliability of the structure for the application of aluminium foam in PCM-based heat storage applications. A 1% increase in the oxide content has been found when the oxide content is examined through EDS. PCMs accumulations are found in pore wall ruptures and microcracks, which are shown in Figure 16,

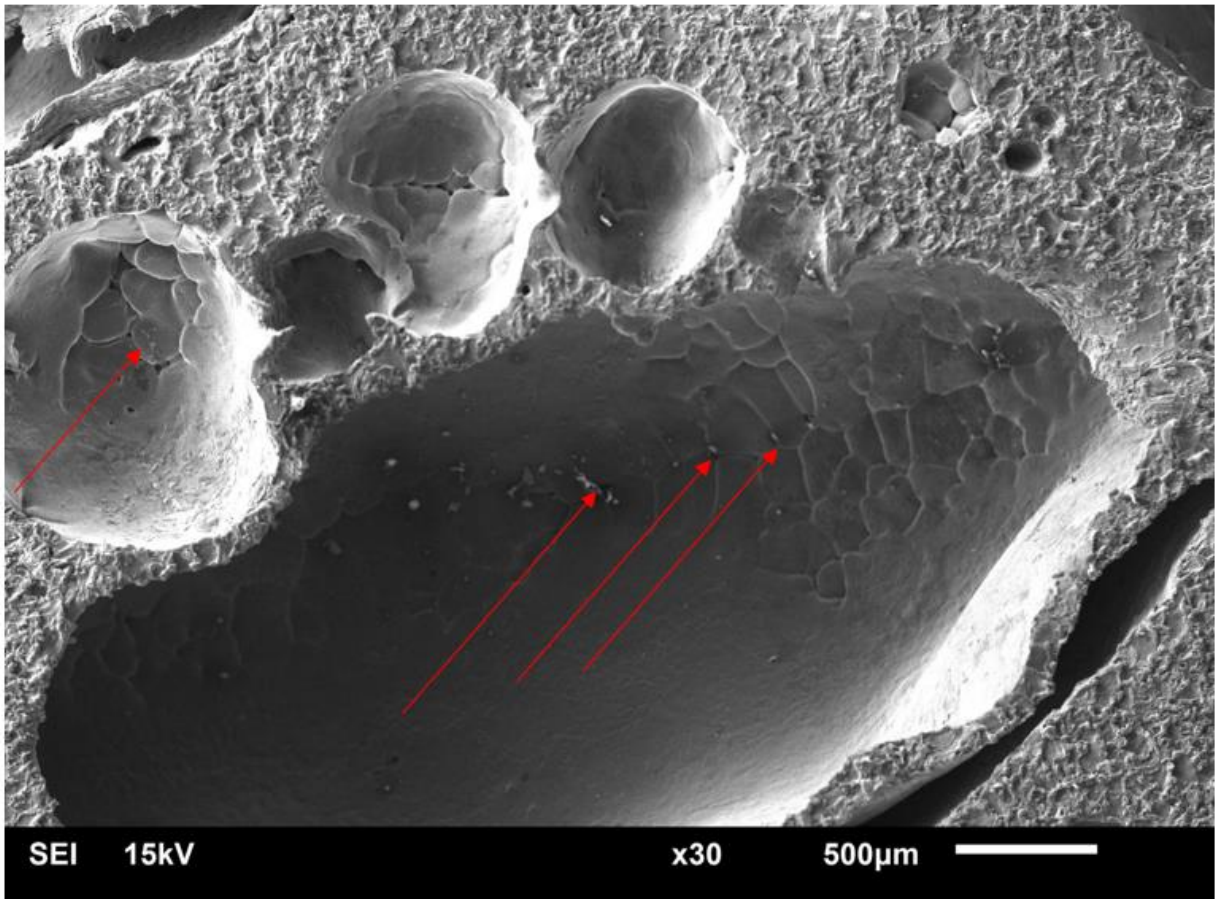

Figure 16. SEM images of PCM agglomerated at pore wall ruptures (marked with red arrows)

This pore wall rupture helps to move the PCM inside the aluminium foam. The heating and cooling cycle of the PCM, with and without aluminium foam, are recorded. The rapid heating and cooling cycles are performed using the hot and cold-water bath from 45 ℃ to 3 ℃. The time taken for the starting and end phase change of both aspects of RT28HC is averaged. It reveals that 40 seconds of time enhancement has been observed for reaching the temperature from 25.1 ℃to 28.1 ℃.

In addition to the time delay, the supercooling degree is reduced with the addition of al foam. It is shown in the graph (Figure 17). Verification is done by conducting the cooling cycle experiment one more time in the range of 40- 25 °C (slightly above the melting point).

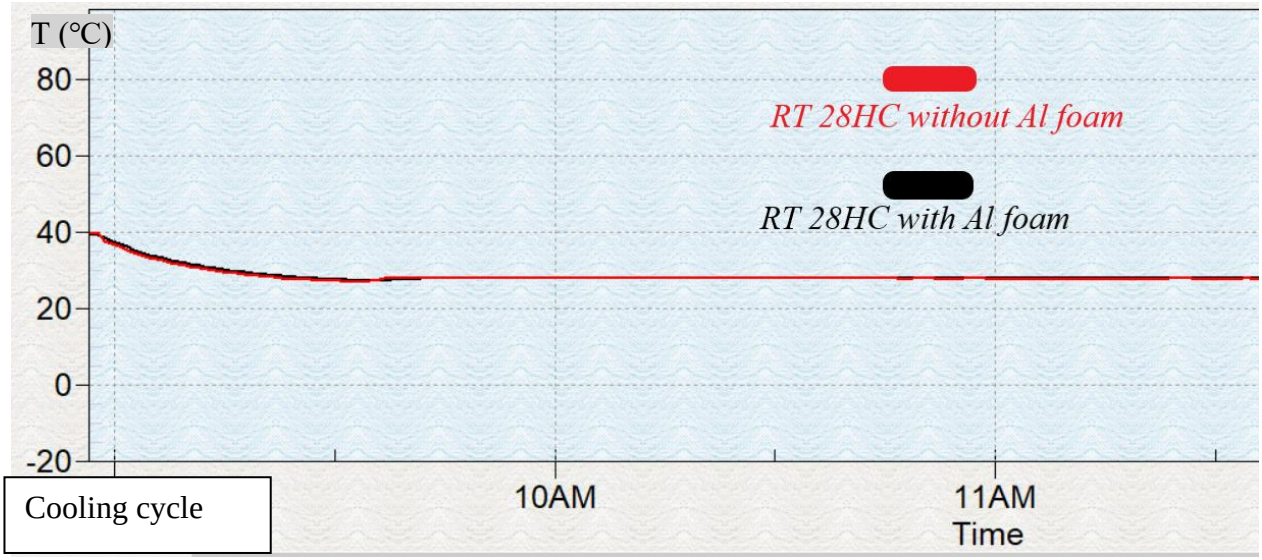

Figure 17. Cooling curve traced by RT28HC with and without Al foam presence

From the graph (Figure 17), it has been found that the solidification point for both samples is 27.3 °C. When a closer examination is made at the solidification point, the degree of supercooling at the test tube RT28HC without Al foam is 0.2 °C. At the same time, the test tube containing the combination of Al foam and RT28HC PCM does not trace the supercooling. It shows that the presence of Al foam neglects the supercooling formed in the RT28HC PCM. It proves that the porous morphology with different pore formation structures provides better support for the PCM to study its compatibility for avoiding phase segregation, supercooling, etc.

The PCM's slower melting is found in the pore wall cavity when the melting at the aluminium foam area is observed. The cavity of the pore wall and the SEM image of the pore wall are presented in the following (Figure 18).

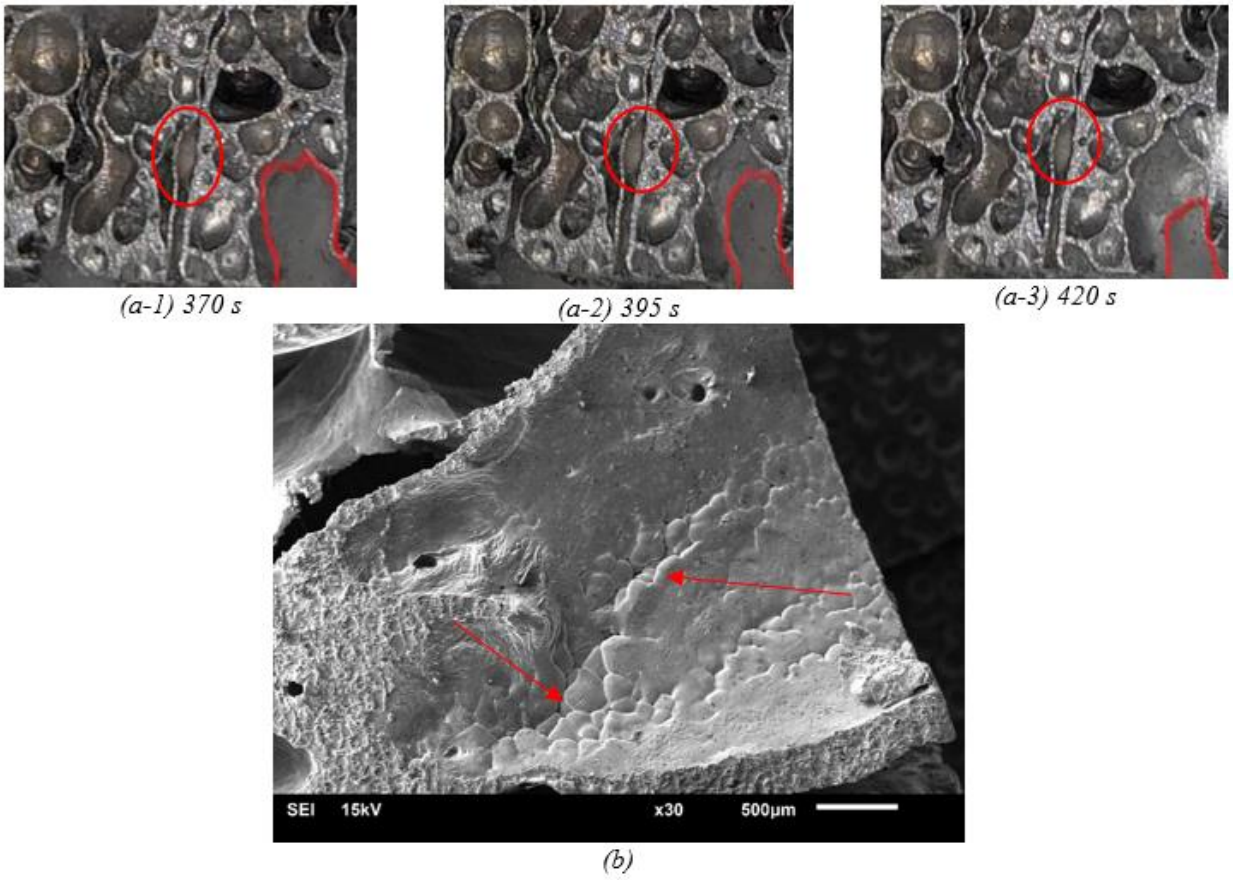

Figure 18. ((a-1)-(a-3))Melt front(marked with red arrow) tracked inside the pores at 370, 395 and 420 s of the heating cycle containing (b)SEM image of the thinner pore walls with microcracks.

The thinner pore walls having numerous ruptures with micro-cracks (Figure 18-b) delay the melting of the PCM compared to the spherical pores due to its non-uniform heat flux generated at the pore walls. It is more commonly visible when the PCM is filled inside the bigger pores having thinner pore walls. At the same time, the other pores have already melted the PCM in their pore cavity. The usage of high-density aluminium foam with fewer macropores(Pore space distance > 1 mm) will limit this non-uniform heating of the PCM. It benefits uniform heat liberation with a more significant heat transfer rate. The PCM deposited at the pores' interconnection contains more PCM(Figure 18, a-1,2,3), delaying the melting even with their higher convective surface area.

4.3.1 Numerical study

Based on the calculated thermophysical properties, the interaction of PCM RT28HC with aluminium foam made of Al-1050 alloy is studied in this section. When the overall heat flux is

analysed, it has been found that the metallic foam structure experiences a non-uniform heat flux rate, but the filled PCM experiences heat flux at a uniform rate. By adjusting the visibility, the non-uniformity of the heat flux rate is found by the solid PCM higher at the thick strut areas, shown in Figure 19.

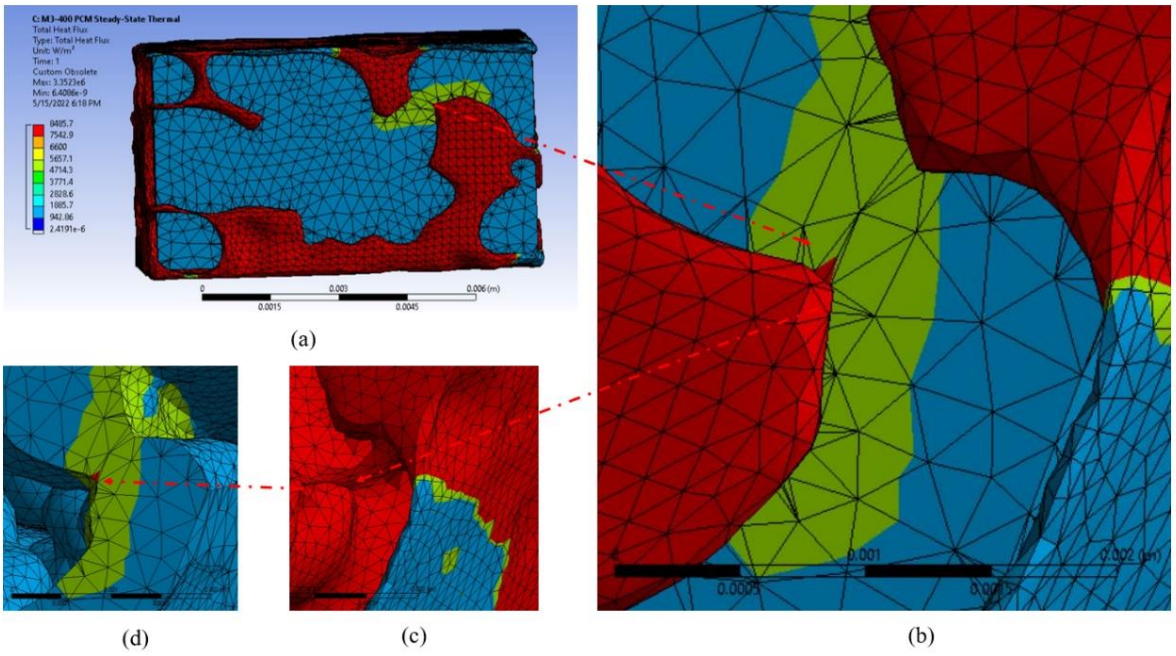

Figure 19 Surrogate model M2 of the aluminium foam filled with PCM (solid-state) (a) obsolete heat flux experienced by the model, (b) area experienced by higher heat flux, heat flux experienced by (c) aluminium foam (8485.7 W/m^2) and (d) PCM (4714.3 W/ m^2)

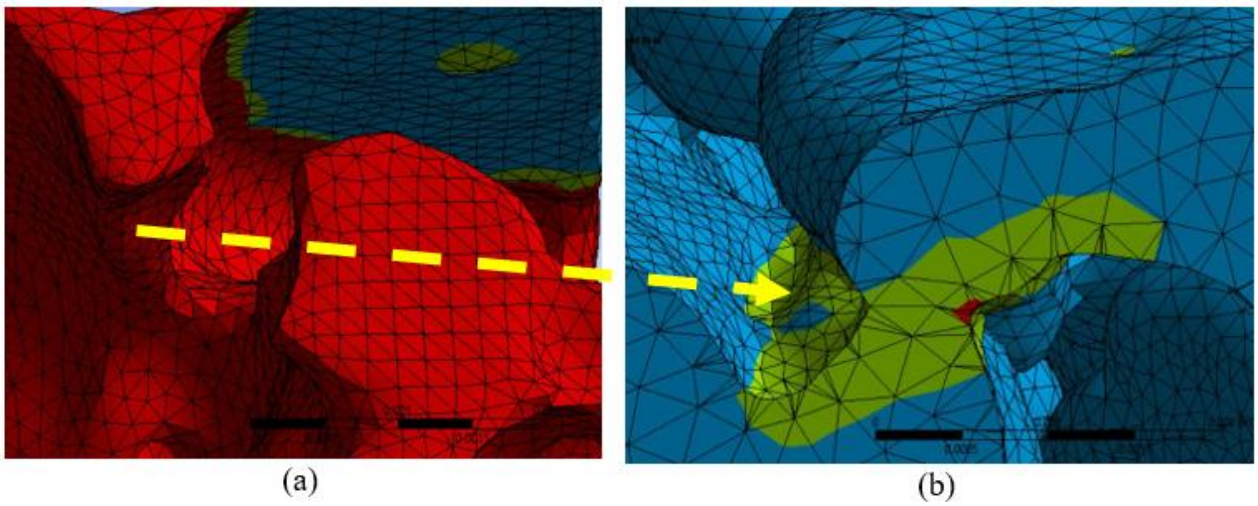

Figure 20. Heat flux experienced by the aluminium foam (8485.7 W/m^2) (a) and the corresponding heat flux experienced by the PCM that is in contact (4714.3 W/ m^2)

The foam structure is essential in determining the amount of heat transfer to the PCM in contact. From the heat transfer analysis of the surrogate model M2, the heat flux rate experienced by the impregnated PCM is 942.86 – 5657.1 W/m^2. The higher heat flux rate is shared by, the thicker strut presence of the aluminium foam, as shown in Figures 19 & 20. It reveals the importance of the morphology of the strut and pores, which experience uneven heat flux for a short period.

From all the numerical studies discussed, the combination of porosity level with the morphology of the pores plays a significant role in deciding the heat transfer rate and the heat flux that results in the melting of the PCM. The numerical results reveal that the PCM's uniform heat transfer rate is achieved at low porosity (< 60 %). At the same time, the structural difference of the strut and the presence of pores alter the heat transfer that melts the PCM quickly compared to the melting in the other areas. It is an essential factor to consider when the temperature gradient of the application is kept low. There is a negligible difference in heating the PCM for a higher gradient. The cooling cycle graph recorded before and after impregnated with the PCM is given below(Figure 21),

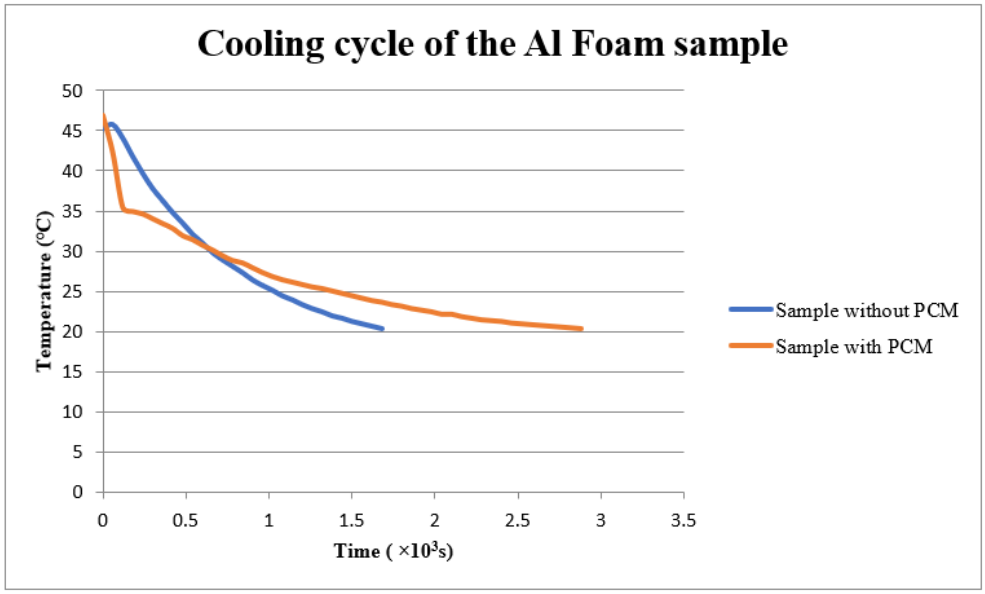

Figure 21. Cooling cycle of the Al foam sample with and without RT28HC

From the graph (Figure 21), the presence of the PCM delays the heat liberation to 1190 s to reach the temperature of 20.3 °C. The present scenario reveals that the PCM impregnated aluminium foam stores an 11.28% higher heat energy. Based on the results, predictions are made

for an aluminium foam panel of 400 × 400 × 10 mm^3 which could be produced to analyse its performance for building applications. Based on the predictions made, the total amount of energy stored corresponding to the porosity is presented in Figure 22.

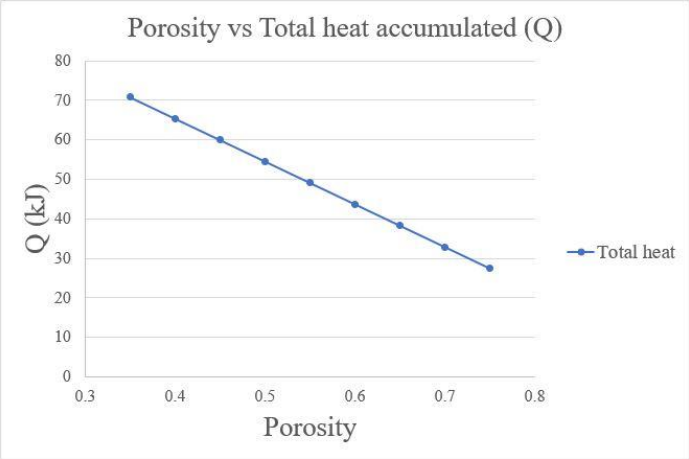

Figure 22. Graph plotting porosity and the corresponding energy stored

The general study is based on the implementation of aluminium foam as a heat transfer medium to achieve better heat storage with PCM. The source of the heat energy is the heat that is brought in from the solar collector. The study reveals the importance of the structural parameters of the aluminium foam in the loading and unloading process of heat energy in PCM. The heat flux experienced by the foam impregnated with PCM is more uniform when the porosity is lower. When the foam panel is considered, the sensible heat storage of the foam is higher than the heat storage of the PCM impregnated inside the foam. Because the temperature gradient in the indoor application is lower, a higher heat transfer rate is needed, which is achieved by using a higher density foam to achieve the complete melting and solidification of the PCM for heat storage. It considers foam panels at a 40-50% porosity level for residential buildings' roofs, ceilings, and domestic heat water supply.

5. LEAKAGE PREVENTION OF THE PCM

PCM leakage reduces performance stability. The porous structure's linked pores prevent PCM leakage during a phase change. Ruptures and microcracks (Figure 23-a), density differential, and volume expansion of PCM lead to foam surface leaking when impregnated. Experiments show that applying a two-component dispersion of a medium molecular epoxy resin, inorganic pigments and fillers, organic solvents, and polyalkylene polyamine-cured additives to the surface of a heat

exchanger can seal liquid PCM in porous aluminium foam while maintaining its thermal conductivity. This coating layer covered the entire aluminium foam sample. Epoxy resin and Al powder are recommended for preventing leaks (Figure 23-b). Epoxy resin prevents leaks, and Al powder boosts the panel's heat transfer rate.

An extended study on the suggested leakage prevention solution is needed, including the ratio of epoxy resin and Al particles, techniques to achieve uniform resin coating, chemical reaction between PCM and resin mixture and weight increase, and heat transfer rate analysis of resin-coated Al foam with and without PCM impregnation.

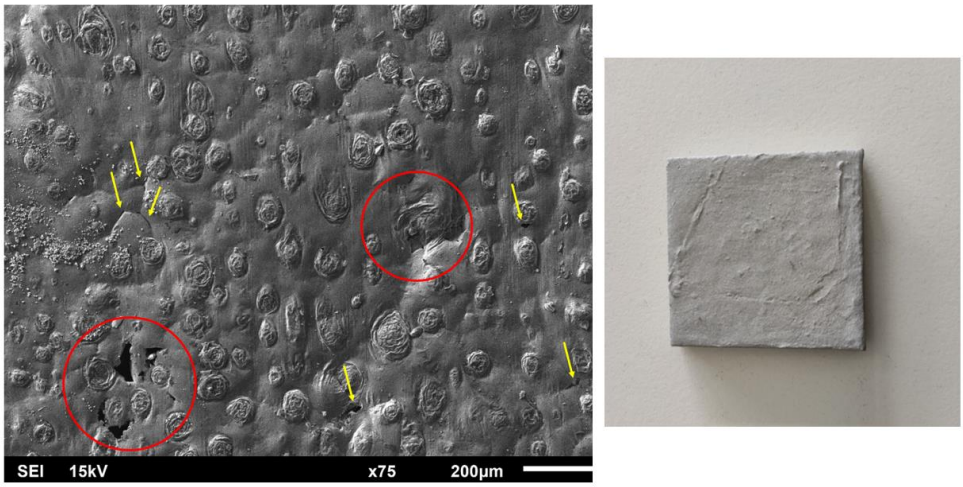

(a) *(b)*

Figure 23. (a) Surface of the aluminium foam with ruptures and microcracks, (b) aluminium foam sample coated with the mixture of epoxy resin and aluminium powder

6. CONCLUSION

This research examines the heat transfer analysis of aluminium foam and the energy balance of PCMs in porous aluminium matrix to build a TES system for enhanced indoor thermal comfort. The study focuses on the production of high-density Al foam of two different alloys, X-ray tomography characterization, image processing for developing surrogate models, modified T-history method for characterizing PCM thermophysical properties, and immersion and thermal performance tests to study PCM interaction with pore walls. The results reveal that Al-1050 with 0.05 wt.% percent TiH_2 will be adequate for greater heat storage with RT28HC PCM (H_m = 242.004 kJ/kg). In addition, the supercooling is avoided with foam insertion and 11.28 % of higher heat storage is achieved.

PUBLICATIONS AND SCHOLARLY WORK

JOURNAL:

1. **GOPINATHAN, Arun.,** JERZ, Jaroslav., KOVÁČIK, Jaroslav., DVORÁK, Tomáš. Investigation of the Relationship between Morphology and Thermal Conductivity of Powder Metallurgically Prepared Aluminium Foams. *In Materials*, 2021, vol. 14, no. 3623. ISSN 1996-1944. https://doi.org/10.3390/ma14133623

   CITED IN: WOS/SCOPUS 1 ×

   - STRĘK, A.M.; DUDZIK, M.; MACHNIEWICZ, T. Specifications for Modelling of the Phenomenon of Compression of Closed-Cell Aluminium Foams with Neural Networks. *Materials* **2022**, *15*, 1262. https://doi.org/10.3390/ma15031262.

CONFERENCE:

1. JERZ, Jaroslav., **GOPINATHAN, Arun**., KOVACIK, Jaroslav. Phase change materials reinforced with aluminum foam for latent heat storage. *In Advanced Materials Letters*, 2021, vol. 12, iss. 3, no. 21031612. ISSN 0976-3961. Available online: https://www.vbripress.com/aml/pdf/1607
2. **GOPINATHAN, Arun**., JERZ, Jaroslav., SIMANČÍK, František., KOVÁČIK, Jaroslav., PAVLÍK, Ľubomír. Assessment of the aluminium foam panel on PCM based thermal energy storage. In: *Conference Proceedings Mechanical teghnologies and structural materials. - Split: Croatian Society for mechanical technologies*, 2019, p. 53-60. ISSN 1847-7917.

   CITED IN: WOS/SCOPUS 1 ×

   - DUARTE, I., FIEDLER, T., KRSTULOVIĆ-OPARA, L. and VESENJAK, M., 2020. Brief review on experimental and computational techniques for characterization of cellular metals. Metals, 10(6), June 2020, Article number 726.
3. JERZ, Jaroslav - SIMANČÍK, František - **GOPINATHAN, Arun** - PUŠKÁR, Anton - SZABÓ, Daniel - ŠPANIELKA, Ján. Aluminium foam based roofing for energy efficient heat recovery from solar gains and maintaining of sufficient thermal comfort in building

interiors. In:*Conference Proceedings Mechanical technologies and structural materials. - Split: Croatian Society for mechanical technologies,* 2019, p. 89-95. ISSN 1847-7917.

4. **GOPINATHAN, Arun.,** JERZ, Jaroslav., KOVÁČIK, Jaroslav. Study of heat transfer characteristics of aluminium foam for PCM-based thermal energy storage applications. In:*Conference Proceedings Mechanical technologies and structural materials. - Split: Croatian Society for mechanical technologies*, 2021, p. 35-42.
5. **GOPINATHAN, Arun.,** JERZ, Jaroslav., KOVÁČIK, Jaroslav., DVORÁK, Tomáš., OROVČÍK, Ľubomír. Study of internal porous structure formation of the powder metallurgically prepared aluminium foam. *In Journal of Physics: Conference Series*. 2021, p. 1-8. doi:10.1088/1742-6596/2045/1/012003
6. JERZ, Jaroslav., **GOPINATHAN, Arun.,** PUŠKÁR, Anton., SZABÓ, Daniel., KOVÁČIK, Jaroslav. Structural design of thermo-active aluminium foam roofing. In:*Conference Proceedings Mechanical technologies and structural materials. - Split: Croatian Society for mechanical technologies*, 2021, p. 53-58.